A Comparison of The Performances of Conventional and Low Salinity Water Alternating Gas Injection for Displacement of Oil

Emmanuel Bucyanayandi[1],* ● **Muhammed Said Ergül[1]** ● **İbrahim Kocabaş[1]** ●

[1] İzmir Kâtip Çelebi University, Department of Energy Engineering, Çiğli Main Campus, İzmir, Türkiye
*Correspondent author: bucyaemmanuel@gmail.com

Abstract

This study focuses on identifying the crucial physical and chemical factors, such as gravity, initial oil phase, injection depth, vertical to horizontal permeability contrast, and salinity of injected water for improving oil recovery factor during water alternating gas (WAG) injection. The conventional WAG injection attracts interest from oil and gas industry and hence, has become one of the most reliable enhanced oil recoveries (EOR) techniques. During WAG injection, due to gravity effect, water subsides below oil layer while gas overflow above the oil layer. In fact, water sweeps bottom zones of the reservoir and gas sweep the attic oil at the upper zones of the reservoir.

Although the conventional WAG does improve oil recovery factor, there still remains a substantial amount of oil in reservoir pores due to rock-fluid and fluid-fluid interfacial tensions (IFT) that leads to the capillary forces impeding the microscopic displacement efficiency. The low salinity waterflooding (LSWF) was therefore proposed to break the IFT between rock clay and fluids, and further increase oil recovery factor. Recent researches revealed that LSWF alters oil-wet reservoir to water-wet behavior. This wettability alteration is believed to be the main mechanism of LSWF to improve oil recovery. Other mechanisms of LSWF include multi-ion exchange (MIE) between rock clay minerals and injected salt water, pH increase, and fines migration. In this study, the CMG GEM simulator was used to simulate conventional WAG injection and LSWAG injection. The simulation results showed that there is an increase of oil recovery factor of about 6% for WAG injection with low salinity water of 1027ppm to sea water of 51,346 ppm. The simulations have also showed that the physical factors namely, gravity, initial oil phase, injection depth, vertical to horizontal permeability contrast are influential on the displacement efficiency and must be studied thoroughly in the design of LSWAG operations besides the salinity and chemical composition of the injection water.

Keywords: Waterflooding; CO_2 flooding; conventional WAG injection; low salinity WAG injection; displacement efficiency of WAG processes

1. Introduction

The economically feasible production of oil is achieved in three stages namely, primary recovery, secondary recovery, and tertiary or enhanced oil recovery. The primary oil recovery

stage refers to the flow of oil from the reservoir into the production wells due to the natural energy/forces that exists in the reservoir. These forces are classified as formation drive due to the compressional energy stored in the oil, connate water and porous formation in the reservoir rock, solution gas drive due the dissolved gas in the oil, gas cap drive due to presence of a gas cap, water drive due to the compressional energy stored in the neighboring large size aquifers, and gravity drive.

The oil recovery factor or the ratio of ultimate cumulative oil production to initial oil in place in the primary stage ranges from 5% to 30%. Secondary recovery methods, namely immiscible waterflooding and gas flooding are usually applied at some stage of primary recovery to enhance and accelerate the production. The additional oil recovery factor due to secondary recovery methods ranges from 5% to 20%. On the average, the total oil recovery factor after primary and secondary recovery methods is between 15% and 40% (Bonder, 2010). The enhanced oil recovery (EOR) methods are applied to recover an additional economically feasible amount of oil that usually remains in the reservoir after primary and secondary recovery methods. Figure 1 shows the partitions of oil recovery percentage by each type of oil recovery methods. It shows that the additional oil recovery factor of 15% to 25% can be achieved by applying EOR methods.
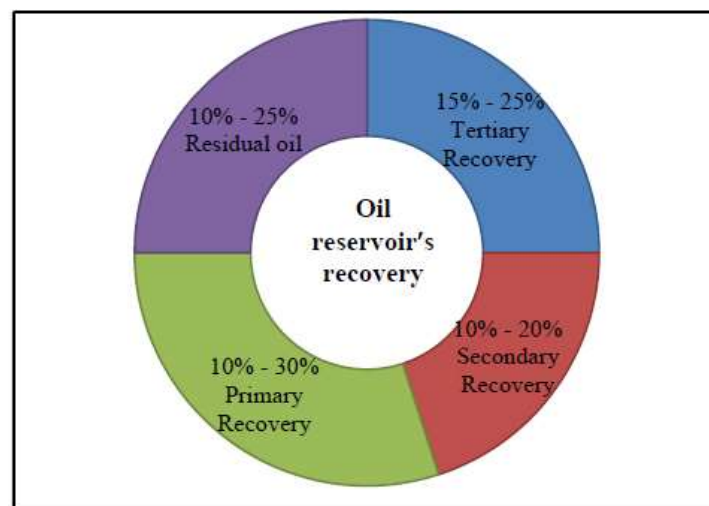
Figure 1. Reservoir oil recovery (Muggeridge et al., 2014; Zitha et al., 2011)

While waterflooding and gas injection are separately considered as secondary oil recovery mechanisms, their combination known as water alternating gas (WAG) injection is referred to as a tertiary or an enhanced oil recovery method. Gas has substantially lower viscosity and density compared to crude oil. Therefore, as a secondary recovery method continous gas injection provides poor macroscopic sweep efficiency due to its high mobility ratio and low density that joinly cause early gas breakthrough (Hustad and Holt, 1992). Therefore, WAG injection was initially used to target improving macroscopic sweep efficiency in gas injection. In fact, conventional WAG injection improves the macroscopic sweep efficiency compared to water flooding and both microscopic and macroacopic displacement efficiency compared to gas injection (Touray, 2013). This improvement is attained by water sweeping the bottom part of the reservoir due to its high-density and gas driving the attic oil due to its low density(Knappskog, 2012). However, the conventional WAG still has its limitations due to strong IFT that hold oil molecules to rock clay surface by multi-valent ions.

Low salinity waterflooding was proposed and applied to improve oil recovery factor further from classical waterflooding. The low salinity waterflooding could increase oil recovery factor from 6 to 12% which takes waterflooding recovery to 8 to 19% orginal oil in place (OOIP) (McGuire et al., 2005). The increase of oil recovery by low salinity water flooding is attributed to four mechanisms: changing the wettability to water wet due to the clay migration; increasing of pH due to $CaCO_3$ that results in wettability alteration; generation of surfactants and reduction of interfacial tension (IFT); multicomponent ion exchange (MIE) between clay minerals and injected brine (Bernard, 1967; Buckley et al., 1989; McGuire et al., 2005).

Low salinity waterflooding changes the reservoir wettability from oil wet to water wet. In other words, low salinity waterflooding affects the oil wet but has no effect on water wet sample. It was found that high concentrations of Ca^{+2} and Mg^{+2} ions in brine formation make the sample more oil wet. Low salinity water flooding also changes the composition of rock and its properties. The experiments showed that the low salinity water dissolves anhydride cements in rock formation. As a result, low salinity water flooding also increases the permeability of reservoir rock (Hamouda and Valderhaug, 2014).

Knowing the effectiveness of conventional WAG and Low Salinity Waterflooding individually, one wonders what could be the performance of low salinity WAG compared to conventional WAG under the influence of other operational and/or design factors such as gravity, initial oil phase, injection depth, and vertical to harizontal permeability contrast. Therefore, this study is aimed to evaluate and compare the performances of conventional WAG injection and LSWAG in improving the oil recovery factor in an 80 ft thick and 1000 ft long sandstone reservoir by considering these factors. These factors are selected and adjusted to evaluate the efficiencies of sea water WAG and low salinity WAG injection. The influence of these factors sequentially on waterflooding, CO_2 gas injection, and WAG injection is investigated with numerical simulations by using CMG-GEM reservoir simulator.

2. Theory of WAG Processes

2.1. Darcy's Law

The flow of fluids in porous medium is governed by Darcy's law. For multiphase flow in porous medium, Darcy's velocity of individual fluid ($\vec{V}_i$) is proportional to effective permeability (k_i) and pressure gradient with gravity effect ($\nabla P - \rho g \nabla d$) and inversely proportional to the viscosity μ_i. In oil reservoirs, velocities of gas, oil, and water are hence calculated by using the flowing Eq. (1), Eq. (2) and Eq. (3) respectively as by Darcy's law.

For gas:
$$\vec{V}_g = -\frac{k_g}{\mu_g}(\nabla P_g - \rho_g g \nabla d) \tag{1}$$

For oil:
$$\vec{V}_o = -\frac{k_o}{\mu_o}(\nabla P_o - \rho_o g \nabla d) \tag{2}$$

For water:
$$\vec{V}_w = -\frac{k_w}{\mu_w}(\nabla P_w - \rho_w g \nabla d) \tag{3}$$

2.2. Relative Permeability

The concept of relative permeability was adopted to express the effective permeability to the base permeability (usually effective permeability to oil at irreducible water saturation). Relative permeability to fluid (k_{ri}) is the ability of medium to conduct that fluid in presence of other fluids. Relative permeability depends on microscopic distribution and saturation of

fluid. It is experimentally correlated with saturation of fluid. The Modified Brooks-Corey (MBC) correlation is a power law model proposed to determine relative permeability for both experimental and field data. Relative permeability is therefore correlated with fluid saturation as shown in the following Eq. (4), Eq. (5) and Eq. (6). (Alpak et al., 1999; Behrenbruch and Goda, 2006; Brooks and Corey, 1964).

$$k_{rw} = k_{rw,max} \left(\frac{S_w - S_{wc}}{1 - S_{or} - S_{wc} - S_{gc}} \right)^{n_w} \qquad (4)$$

$$k_{ro} = k_{ro,max} \left(\frac{S_o - S_{or}}{1 - S_{or} - S_{wc} - S_{gc}} \right)^{n_o} \qquad (5)$$

$$k_{rg} = k_{rg,max} \left(\frac{S_g - S_{gc}}{1 - S_{or} - S_{wc} - S_{gc}} \right)^{n_g} \qquad (6)$$

Where, S_w is water saturation, S_{wc} is irreducible water saturation, S_o is oil saturation, S_{or} is residual oil saturation, S_g is gas saturation, S_{gc} is irreducible gas saturation, n_w, n_o, and n_g refer to corey exponents and they range from 1 to 6, and $k_{rw,max}$, $k_{ro,max}$, and $k_{rg,max}$ are the maximum or end point relative permeabilities.

3. Theory of the Mechanisms of Low Salinity Waterflooding

Low salinity waterflooding is a technique of injecting water with low concentration of salts between (salinity: 1000-2000 ppm). It is a chemical technique that was recently adopted to improve oil production. From different experimental analysis of core flooding, chemical changes of rock and fluids due to low salinity flooding are the main reason of oil recovery improvement. The mechanism of low salinity waterflooding is based on breaking the electric forces exhibited by high salinity formation water to oil to rock surface. Hence, certain conditions that include the presence of clay minerals like calcite and dolomite and the polarity of oil, they are the key conditions for effectiveness of low salinity waterflooding (Bernard, 1967; Tang and Morrow, 1999). The following are the main mechanisms by which low salinity waterflooding improve the oil displacement in the reservoir:

3.1. Multicomponent Ion Exchange (MIE)

In the reservoir, oil is attached to rock surface by bonding to multivalent cations. By injecting the low salinity water, K^+ and Na^+ ions replace these multivalent ions like Ca^{2+} and Mg^{2+}. As a result, the oil is released from rock surface in the form of calcium or magnesium carboxy complex. Unlike for high salinity water that strengthen the oil bonding to clay, injection of low salinity water weakens these bonding for ion exchange to occur. The effectiveness of low salinity water flooding therefore depends on composition of water formation and injection brine.
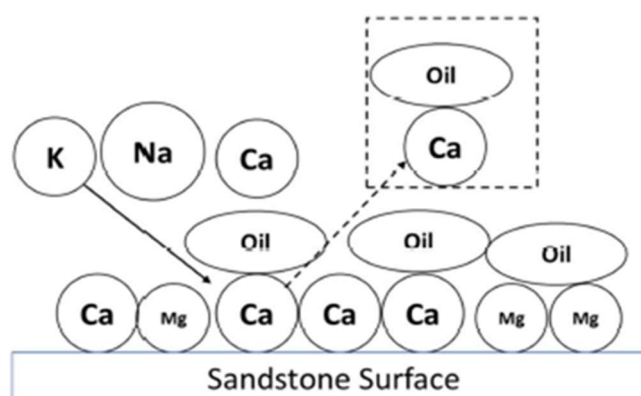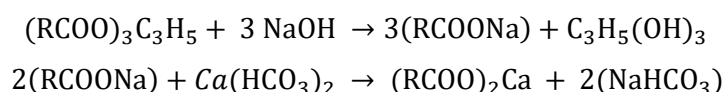
Figure 2. Low salinity mechanisms of multiple ions exchange (MIE) with potassium replacing calcium and liberation of oil in the form of calcium carboxylate complex, modified after (Srisuriyachai and Muchalintamolee, 2014).

3.2. Wettability Alteration

According to different researches, low salinity water injection changes the wettability. The low salinity waterflooding alters the reservoir from oil wet to water wet. It was obtained that low salinity waterflooding affect the oil wet and it has no effect on water wet sample. It was found that high concentrations of Ca^{2+} and Mg^{2+} ions in brine formation make the sample more oil wet. The effect of reservoir rock mineralogy on the application of low salinity water was also reviewed. Low salinity waterflooding therefore changes the composition of rock and its properties. The experiments showed that the low salinity water dissolves anhydride cements in rock formation. As the result, low salinity water flooding increases the permeability of reservoir rock (Tang and Morrow, 1999).

3.3. Increased pH Effect and Reduced Interfacial Tension (IFT)

Low salinity water flooding leads to generation of hydroxyl ions to reactions with rock minerals. This causes the pH increase from 7 to 8 and even to 9. In fact, low salinity waterflooding like alkaline flooding reduces the interfacial tensions between oil and rock and increases pH. The IFT are the forces that hold oil into pore spaces. The increase of pH and reduction of interfacial tensions between reservoir rock and fluids alter the rock to more water wet and hence improve oil recovery. In addition, oil with its chemical structure, the increase of pH facilitates the in-situ surfactant generation by saponification reactions as shown below (McGuire et al., 2005). In this case, low salinity water flooding acts like surfactant flooding and cause oil dispersion into water.

$$(RCOO)_3C_3H_5 + 3\,NaOH \rightarrow 3(RCOONa) + C_3H_5(OH)_3$$

$$2(RCOONa) + Ca(HCO_3)_2 \rightarrow (RCOO)_2Ca + 2(NaHCO_3)$$

4. Methodology

The CMG-GEM one of the reservoir simulators developed by Computer Modeling Group (CMG) was used to simulate different scenarios of waterflooding, gas injection, and WAG injection. GEM is a generalized equation of state model reservoir simulator, i.e., it is an equation of state compositional simulator for multi-component reservoir fluids. GEM is used to simulate all the processes involving chemical change in the reservoir but at a constant temperature.

4.1. Reservoir and Fluids Modelling

The actual data from the Cranfield oil field reservoir and some assumptions were considered to model the reservoir and formation fluids. As published in the Mississippi oil and gas board (MOGB) publication in 1966, Cranfield oil field was discovered in 1943, its reservoir has a geological dome with gas cap, oil ring and water at different depths (Mississippi Oil and Gas Board, 1966). Until 1966, the total oil and gas production was at least 37mmbbl and 672 bscf respectively, then the reservoir was subjected to secondary oil recovery by water drive in 2005, and with enhanced oil recovery by CO_2 flooding in 2008 at some part of the field (Hovorka et al., 2008). A CO_2 sequestration test was also carried out in Cranfield pilot size of 9400 ft x 8400ft with net pay of 80ft (Delshad et al., 2013; Hosseini et al., 2013). In this study, the reservoir model in Table 1 was built by using the data published on Cranfield oil field reservoir.

Table 1. Reservoir model

Parameter	Value
Reservoir size (ft)	1000 x 100x 80
Number of grid blocks	20x1x8
Reservoir depth (ft)	9950
Reservoir Temperature (°F)	257
Initial oil saturation	0.6
Initial Pressure (psi)	4650
Salinity, TDS (ppm)	150,000

By using GEM builder and Winprop, a reservoir model was built by inputting the data to be processed by CMG-GEM. The dimension of the reservoir model is 1000 ft x 100ft x 80ft. In fact, as shown in Figure 3, the two-dimensional (2D) reservoir model was considered with single injector well and producer well pattern.
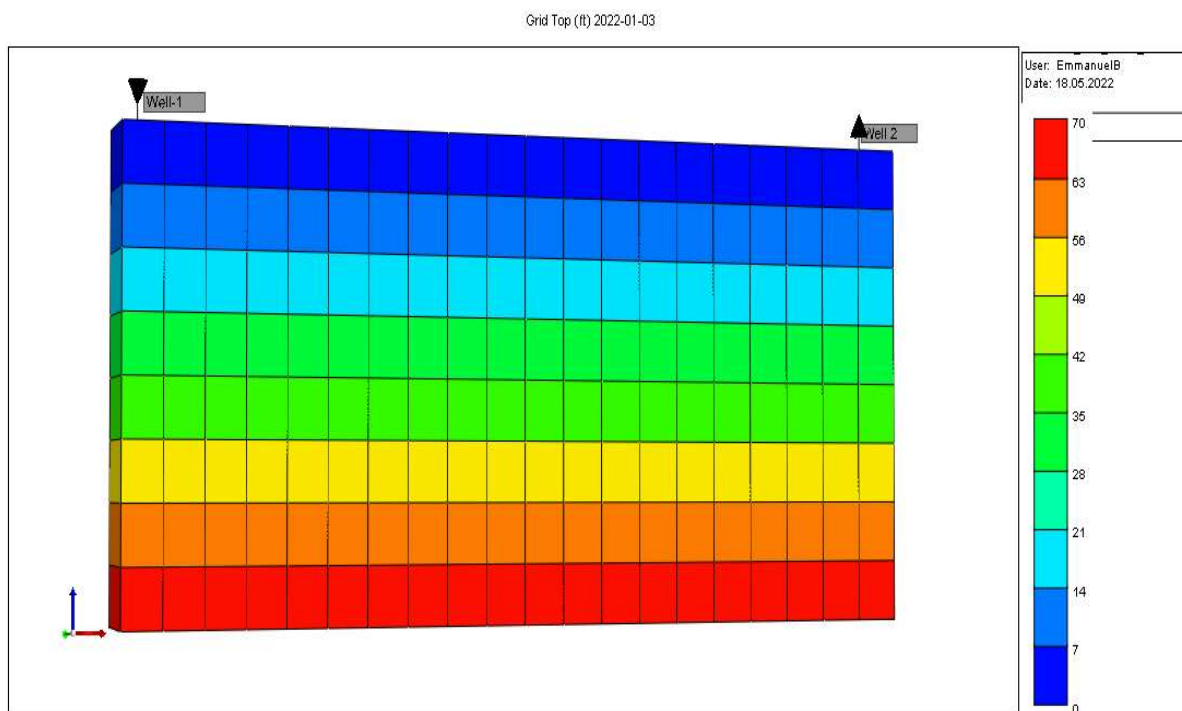

Figure 3. Reservoir model with single injector and producer wells

Reservoir fluids model was built by using the data of composition of reservoir fluids as also published in MOGB publication, 1966 (Mississippi Oil and Gas Board, 1966). The composition of reservoir fluid is shown in Table 2. The two-phase envelope in Figure 4 shows that the crude oil is in two phases (liquid and gas) at initial conditions of 4650 psi and 257 °F.

Table 2. Reservoir Fluid Composition (Mississippi Oil and Gas Board, 1966).

Component	Composition (Mol Fraction)
CO_2	0.0184
CH_4	0.5376
C_2H_6	0.0717
C_3H_8	0.0334
IC_4	0.0104
NC_4	0.0158
IC_5	0.0123
NC_5	0.0095
NC_6	0.0248
C_{7+}	0.2661
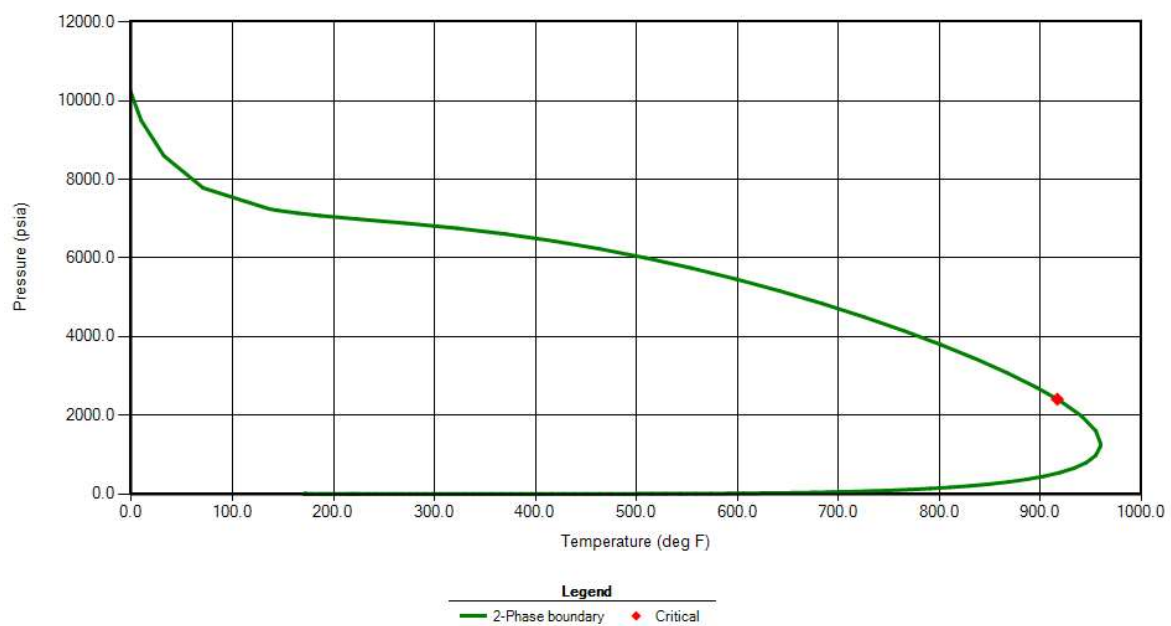
Figure 4. The two-phase envelope for crude oil initially in two phases using Peng-Robinson EOS

The relative permeability data in Table 3 were used for this reservoir and assumed for high salinity waterflooding. Brooks-Corey correlation was then applied to model and produce the oil-water and liquid-gas relative permeability curves.

Table 3. Rock and fluid parameters for relative permeability curves of the base case (Delshad et al., 2013; Hosseini et al., 2013)

Rock-fluid parameters	Values
k_{rwo}^0: k_{rw} at irreducible oil	0.5
k_{row}^0: k_{ro} at connate water	0.65
$k_{rgw}^0 = k_{rgo}^0$: k_{rg} at connate liquid	0.8
S_{org}: endpoint saturation (residual oil for gas liquid table)	0.15
$S_{wrg} = S_{wro}$: endpoint saturation (connate water)	4.0
S_{orw}, endpoint saturation (residual oil for water oil table)	0.2
$S_{grw} = S_{gro}$: endpoint saturation (connate gas)	0.075
n_{1wo} : exponent for calculating k_{rw}	4.0
$n_{1wg} = C_{1og}$: exponent for calculating k_{rog}	4.0
n_{1ow}: exponent for calculating k_{row}	2.38
$n_{1gw} = C_{1go}$: exponent for calculating k_{rg}	2.2

4.2. Geochemical Reactions Modelling

The geochemical reactions were modelled by using the data taken from different literatures. The Cranfield oil reservoir is a Lower Tuscaloosa Formation (LTF) that is locally referred as "D-E sand". The LTF is mainly composed of quartz (79.4%), chlorite (chamosite) (11.8%), kaolinite (3.1%), and illite (1.3%). There is also the presence of soluble and active minerals like calcite (1.1%), dolomite (0.4%), and albite (0.2%). On the other hand, the Tuscaloosa formation brine is a Na-Ca-Cl water type. The average salinity of the formation water is measured as 150000ppm (Total Dissolved Solids, TDS) and its pH is 5.7 (Lu et al., 2012; Soong et al., 2016; Stancliffe and Adams, 1986). Table 4 shows the ionic composition of the formation brine used.

Table 4. Mineral composition of Lower Tuscaloosa Formation brine (Soong et al., 2016)

Ions	Concentration (ppm)
Ca^{2+}	11798
Mg^{2+}	1035
Na^+	43743
SO_4^{2-}	238
Cl^-	92223

The data for synthetic sea water were taken from experimental research by Teklu et al., 2017. Low salinity water was hence modelled by diluting sea water 2 times, 4 times and 5 times (Teklu et al., 2017). The ions concentration of injected sea water and low salinity water are illustrated in Table 5.
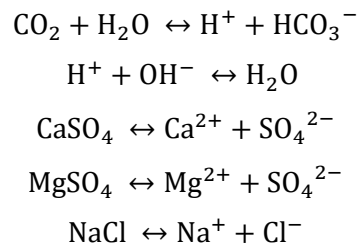
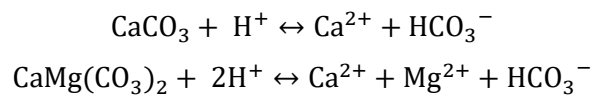**Table 5.** Concentration of ions of brine and low salinity water used for simulation

Ions	Sea Water (ppm)	LoSal1 (ppm)	Losal2(ppm)	LoSal3(ppm)
Ca^{2+}	691.5	346	173	13.7
Mg^{2+}	3459.0	1729.5	864.9	69.2
Na^+	1286.1	6495.1	3247.6	259.8
SO_4^{2-}	4098.8	2049.8	1024.9	82.1
Cl^-	30110.6	15058.7	7529.7	602.1
TDS	**51346**	**25679.1**	**12840.1**	**1026.9**

The injection of water with different salinity content to formation brine affects the rock-brine-oil system interfaces equilibrium and causes chemical change in the reservoir. Software packages like WOLERY and PHREEQC were programed for this geochemistry. These databases were therefore used through Process Wizard interface provided in GEM simulator to model the aqueous, mineral, and ion exchange reactions. These chemical reactions are reversible according to ions concentration in injected water.
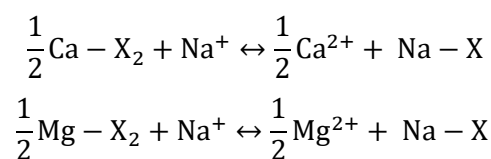
Aqueous Reactions:

$$CO_2 + H_2O \leftrightarrow H^+ + HCO_3^-$$

$$H^+ + OH^- \leftrightarrow H_2O$$

$$CaSO_4 \leftrightarrow Ca^{2+} + SO_4^{2-}$$

$$MgSO_4 \leftrightarrow Mg^{2+} + SO_4^{2-}$$

$$NaCl \leftrightarrow Na^+ + Cl^-$$

Mineral Reactions:

$$CaCO_3 + H^+ \leftrightarrow Ca^{2+} + HCO_3^-$$

$$CaMg(CO_3)_2 + 2H^+ \leftrightarrow Ca^{2+} + Mg^{2+} + HCO_3^-$$

Ion Exchange Reactions:

$$\frac{1}{2}Ca - X_2 + Na^+ \leftrightarrow \frac{1}{2}Ca^{2+} + Na - X$$

$$\frac{1}{2}Mg - X_2 + Na^+ \leftrightarrow \frac{1}{2}Mg^{2+} + Na - X$$

In these ion exchange reactions, Na^+ is taken up by the exchanger X on the clay surface. In case of low salinity water injection, multivalent ions like Ca^{2+} and Mg^{2+} dissolute with carboxylate group from the clay surface and exchange with mono-valent ions like Na^+ and K^+.

For these ion exchange reactions on clay surface are measured by equivalent fractions $\zeta(Na - X)$, $\zeta(Ca - X_2)$, and $\zeta(Mg - X_2)$. Therefore, ion exchanges are modelled by selectivity coefficients which are operational variables as shown in Eq. (7) and Eq. (8) (Dang et al., 2013; Dang et al., 2015; Dang et al., 2016; Gaines and Thomas, 1953; CMG-GEM)

$$K'_{Na/Ca} = \frac{\zeta(Na - X)[m(Ca^{2+})]^{0.5}}{[\zeta(Ca - X_2)]^{0.5}m(Na^+)} \times \frac{[\gamma(Ca^{2+})]^{0.5}}{\gamma(Na^+)} \tag{7}$$

$$K'_{Na/Mg} = \frac{\zeta(Na - X)[m(Mg^{2+})]^{0.5}}{[\zeta(Mg - X_2)]^{0.5}m(Na^+)} \times \frac{[\gamma(Mg^{2+})]^{0.5}}{\gamma(Na^+)} \tag{8}$$

Where, m is the ion concentration and γ is the activity coefficient. In GEM, a parameter Cation Exchange Capacity (CEC) was introduced to measure the number of ions adsorbed on clay surface by ion exchange. Hence, the total number of moles of $Na - X$, $Ca - X_2$, and $Mg - X_2$ are calculated for total grid bulk volume (V) as shown in Eq. (9).

$$V\varphi(CEC) = VN_{Na-X} + 2VN_{Ca-X_2} + 2VN_{Mg-X_2} \tag{9}$$

The number of moles of $Na - X$, $Ca - X_2$, and $Mg - X_2$ per grid block are therefore calculated by dividing the bulk volume as indicated in Eq. (10).

$$\varphi(CEC) = N_{Na-X} + 2N_{Ca-X_2} + 2N_{Mg-X_2} \tag{10}$$

Consequently, equivalent fractions are calculated as in the following Eq. (11), Eq. (12) and Eq. (13).

$$\zeta(Na - X) = \frac{N_{Na-X}}{\varphi(CEC)} \tag{11}$$

$$\zeta(Ca - X_2) = \frac{N_{Ca-X_2}}{\varphi(CEC)} \tag{12}$$

$$\zeta(Mg - X_2) = \frac{N_{Mg-X_2}}{\varphi(CEC)} \tag{13}$$

4.3. Wettability Alteration Model

Wettability alteration due to LSWF is modelled by shifting relative permeability curves to water wetting conditions. Normally relative permeability data for simulation are measured through core analysis experiments. However, in this study, relative permeability data are assumed for formation brine and the rock is considered oil wet. Therefore, relative permeability curves for LSWF were obtained by reducing S_{or} from 0.2 to 0.14 but the curvature was not changed as shown in the Figure 5.

From these two sets of relative permeability curves, it is required to perform an interpolation for oil-water relative permeability for different salinity water injections. Relative permeability changes because the adsorption, dissolution, or precipitation that take place during salty water injection. The ion exchange equivalent fraction one of the options provided by GEM was selected for oil water relative permeability curves interpolations. The ion exchange equivalent fraction is preferred because it includes ion exchange as the main mechanism of low salinity waterflooding. It was assumed in this study that if the initial equivalent fraction $\zeta(Ca - X_2)$, is greater than 0.4, the relative permeability curves for high salinity is used and if it is less than 0.19, then those for low salinity are used. The initial equivalent fraction $\zeta(Ca - X_2)$, between 0.4 and 0.19, the interpolation is then performed.
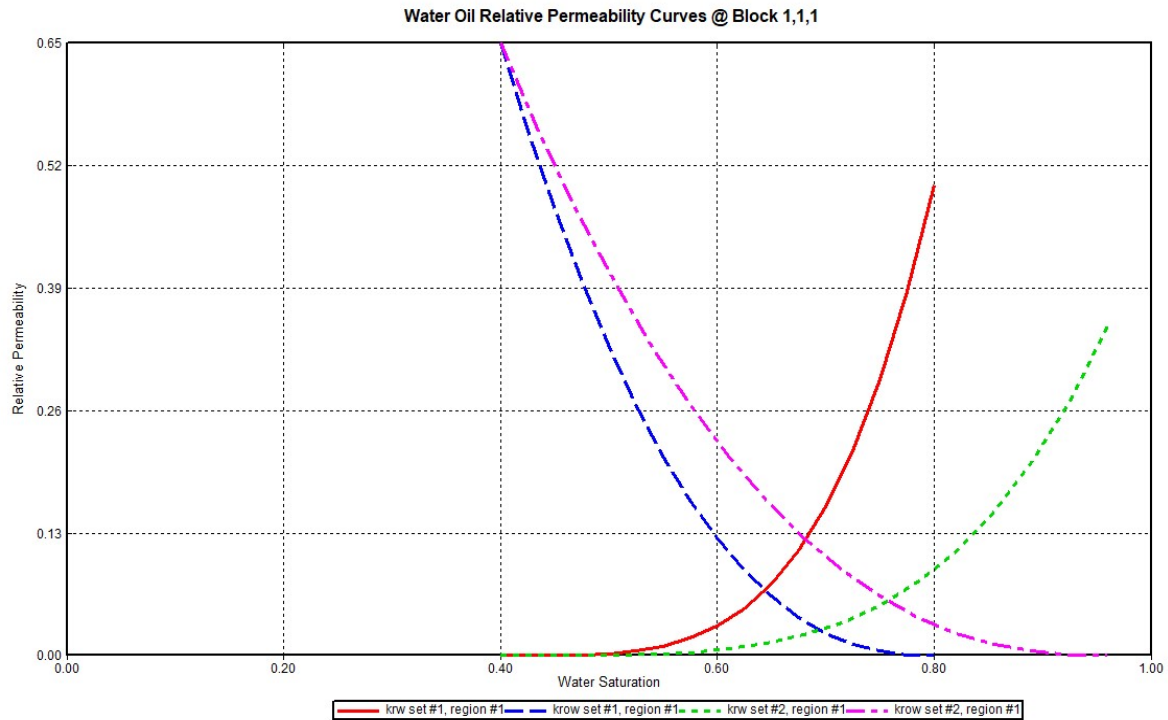
Figure 5. Wettability alteration modeling by shifting relative permeability curves from oil wet to water wet behavior

The Eq. (14) demonstrates how the interpolant for ion exchange is calculated as proposed in these research studies (Egbe et al., 2021; Jerauld et al., 2008; Qiao et al. , 2015).

$$\omega = \frac{\zeta(Ca - X_2) - \zeta(Ca - X_2)^{HSW}}{\zeta(Ca - X_2)^{LSW} - \zeta(Ca - X_2)^{HSW}} \tag{14}$$

Relative permeability values can then be calculated by linear interpolation as shown in the following Eq. (15) and Eq. (16).

$$K_{rw} = \omega K_{rw}^{LSW} + (1 - \omega) K_{rw}^{HSW} \tag{15}$$

$$K_{ro} = \omega K_{ro}^{LSW} + (1 - \omega) K_{ro}^{HSW} \tag{16}$$

Where, K_{rw} and K_{ro} are water and oil relative permeability for injected brine respectively, K_{rw}^{HSW} and K_{ro}^{HSW} are water and oil relative permeability for formation brine respectively, K_{rw}^{LSW} and K_{ro}^{LSW} are water and oil relative permeability of low salinity water respectively.

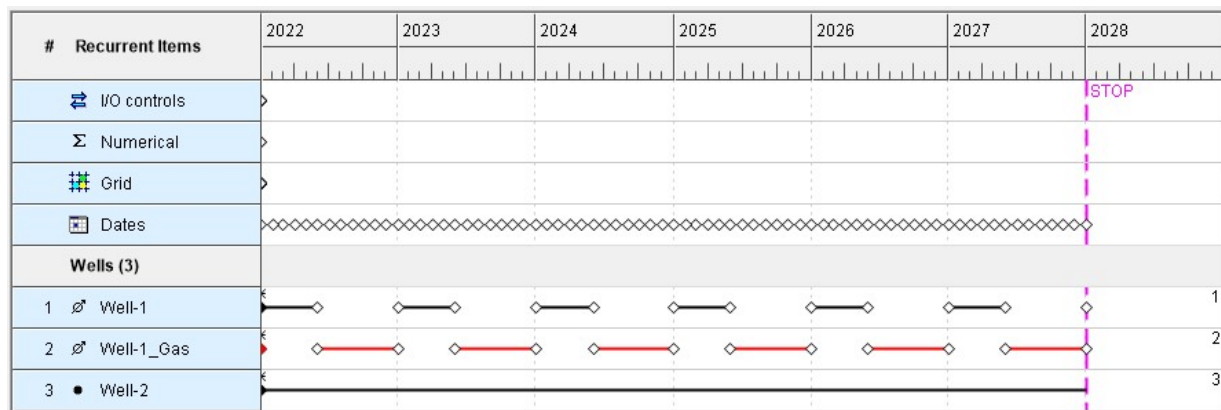## 4.4. Waterflooding and CO2 Gas Flooding Modelling

The waterflooding was modelled by using Process Wizard interface in builder that was provided for modelling the processes that involve geochemical changes. The maximum bottom hole pressure of 5500 psi and the maximum surface water rate (SWR) of 100bbl/day were set as the injector well constraints. The CO_2 gas that was already modelled in the components of crude oil was selected as the injected fluid. The maximum bottom hole pressure of 5500 psi was also set as the injector well constraint with surface gas rate (SGR) of 100000 ft³/day. The producer well constraints for both waterflooding and CO_2 gas flooding were the minimum bottom hole pressure of 4060 psi and the surface oil rate (STO) of 200bbl/day. The simulations were run for 6 years continuously. The parameters in Table 6 were used in order to evaluate and compare the oil sweep efficiencies.

Table 6. Operational parameters for Waterflooding and CO_2 gas injection simulations

Parameters	Waterflooding	CO_2 gas injection
Initial phase of oil	• Two phases (liquid-gas) • Single phase (liquid)	• Two phases (liquid-gas) • Single phase (liquid)
Injection Depth	• All zones • Upper zones	• All zones • Lower zones
Vertical Permeability	• 50 md • 10 md	• 50 md • 10 md

4.5. Conventional WAG and LSWAG Modelling

The typical WAG injection was modelled by injecting both water and CO_2 gas at the same injector well. The injector well was open and shut-in alternately after each six month for 6 years. The figure 6 is the graphical illustration of the WAG model created.
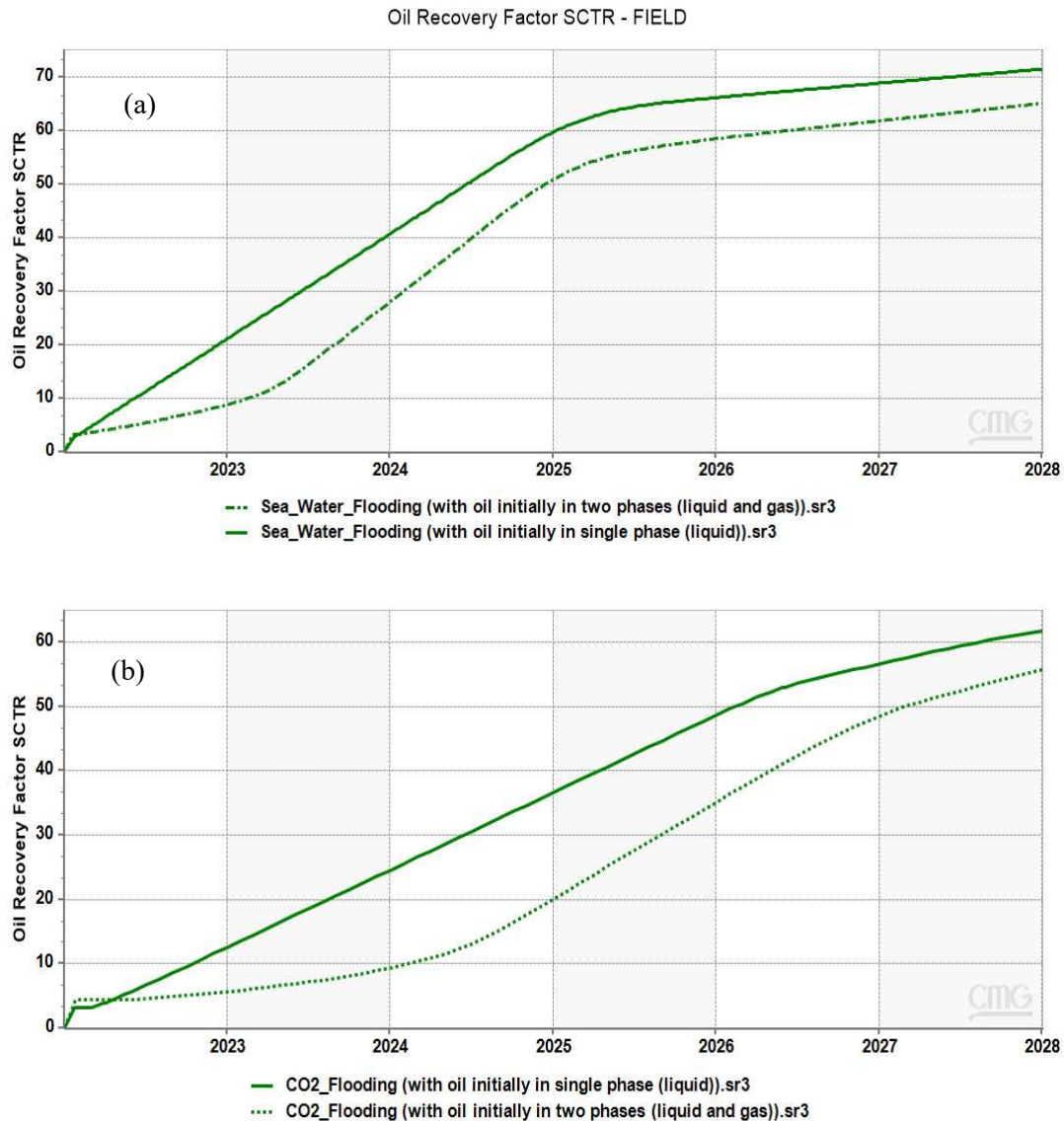

Figure 6. Graphic Model of WAG injection

5. Results and Discussion

5.1. Effect of initial phase of reservoir fluid

The effect of initial phase of crude oil was evaluated by simulation of waterflooding and CO_2 gas injection separately. Due to high mole fraction of methane compared to those of other components, oil was initially found to exist in two phases (liquid and gas) as shown in Figure 4. Mole fraction of oil components was therefore adjusted to create initial single liquid phase by increasing mole fraction of C_{7+} to 0.4661 and decreasing mole fraction of methane to 0.3376.

Figure 7 illustrates the oil recovery factors comparison with oil initially in single phase and two-phases during sea waterflooding and CO_2 gas injection respectively. The oil recovery factor difference is attributed to the fact that gas oil ratio is high for oil initially in two phases during production. In fact, the high gas production with oil initially in two phases influenced the relative permeabilities and caused to obtain less oil recovery percentage.

Oil Recovery Factor SCTR - FIELD

--- Sea_Water_Flooding (with oil initially in two phases (liquid and gas)).sr3
—— Sea_Water_Flooding (with oil initially in single phase (liquid)).sr3

—— CO2_Flooding (with oil initially in single phase (liquid)).sr3
···· CO2_Flooding (with oil initially in two phases (liquid and gas)).sr3

Figure 7. Effect of initial phase of crude oil on oil recovery factor during (a) waterflooding, (b) CO_2 injection

5.2. Gravity Effect

Figure 8 displays the water and gas saturation on the course of continuing waterflooding and CO_2 gas injection respectively. During waterflooding, water displaces oil from side-bottom of the reservoir from injector to the producer well. In fact, due to gravity effect, water flow down at the lower zones of the reservoir because it is denser than oil. The pressure difference also causes water saturation to increase going forward from the injector well to the producer well. In the case of continued CO_2 gas injection, gravity effect also causes the gas to move to the upper zones of the reservoir from injector well to the producer well.
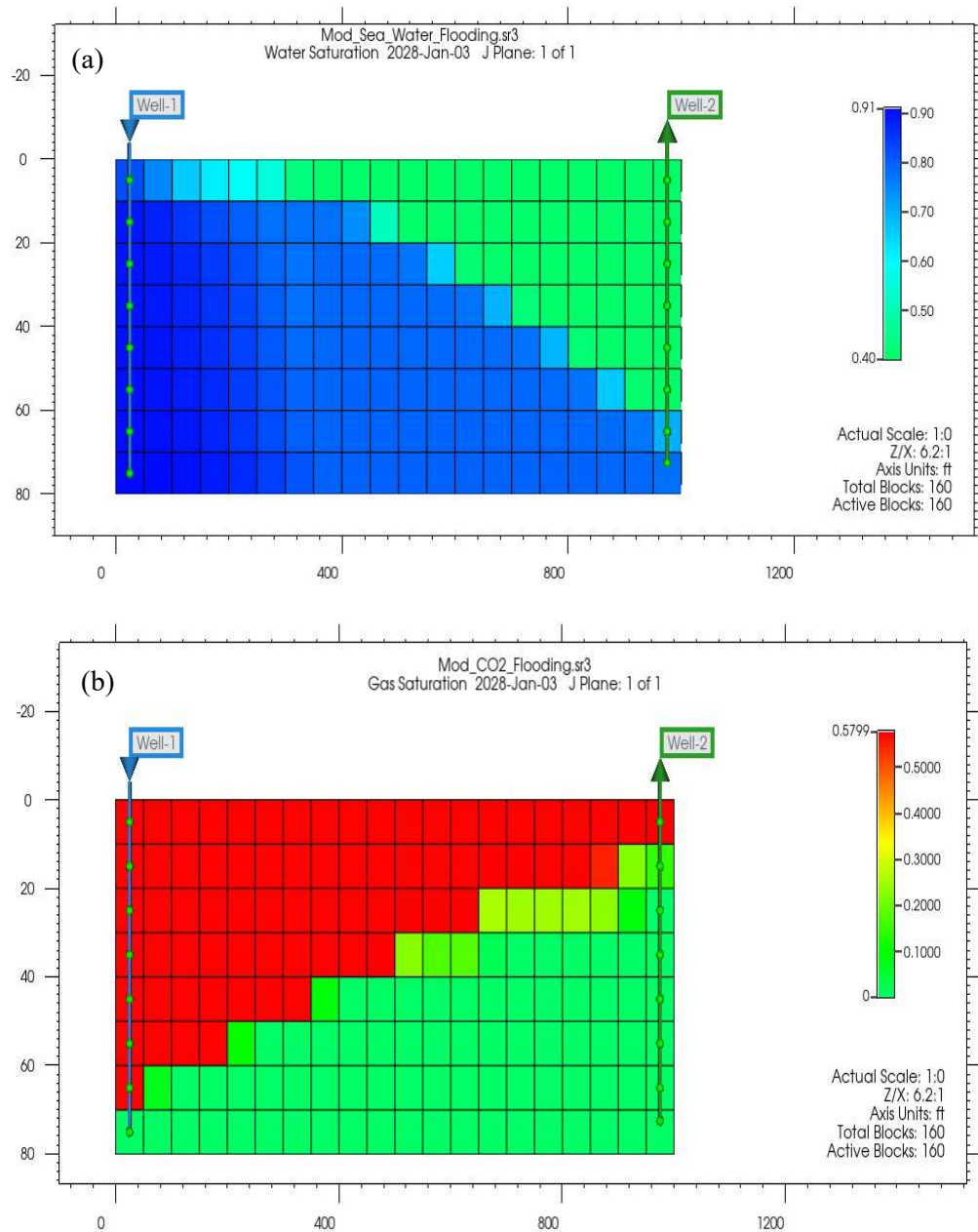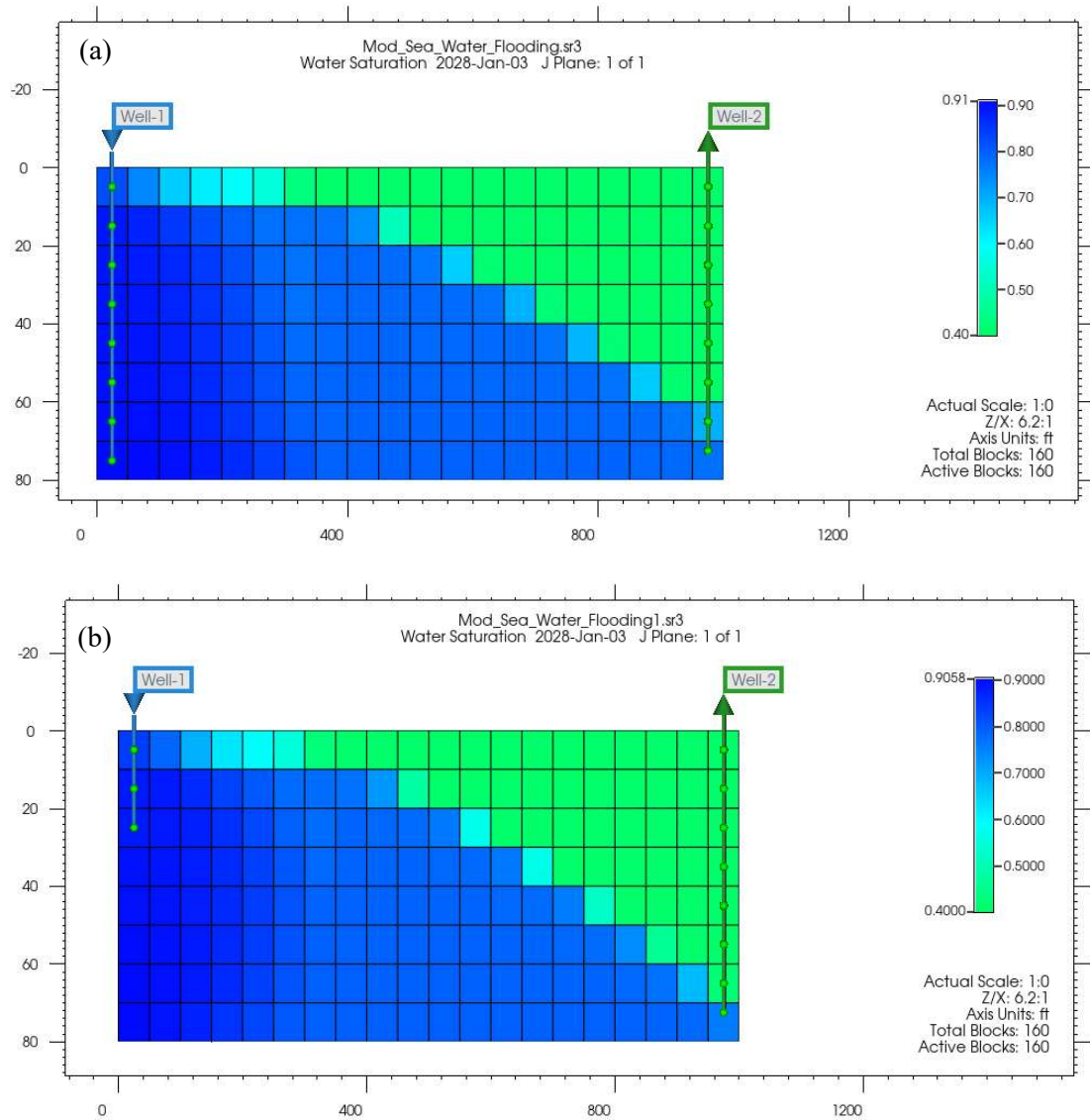
Figure 8. Water saturation during (a) waterflooding, (b) CO_2 gas flooding

5.3. Injection Depth Effect

In order to control the water and gas early breakthrough from lower and upper zones of reservoir respectively, and improve the sweep efficiencies, the adjustment on the injection depth was applied by perforating upper zones for waterflooding and lower zones for gas injection. It was deemed to be of importance to inject water from upper zones to increase the volumetric sweep efficiency by retarding the water breakthrough while favoring the horizontal front displacement of water in upper zones of the reservoir. The graphs in Figure 9 display the comparison between front displacement of water when injected from upper zones and when injected from all zones.

Figure 9. Water saturation profile during waterflooding from (a) all zones, (b) upper zones

On the other hand gas was injected from lower zones of the reservoir to allow gas to contact with oil at the lower and middle zones of the reservoir and eventually prevent early gas breakthrough at the upper zones of the reservoir. Figure 10 below shows the positive impact of injecting gas through perforations in the lower zones; there is an increased region contacted with gas and hence increased the oil sweep efficiency.
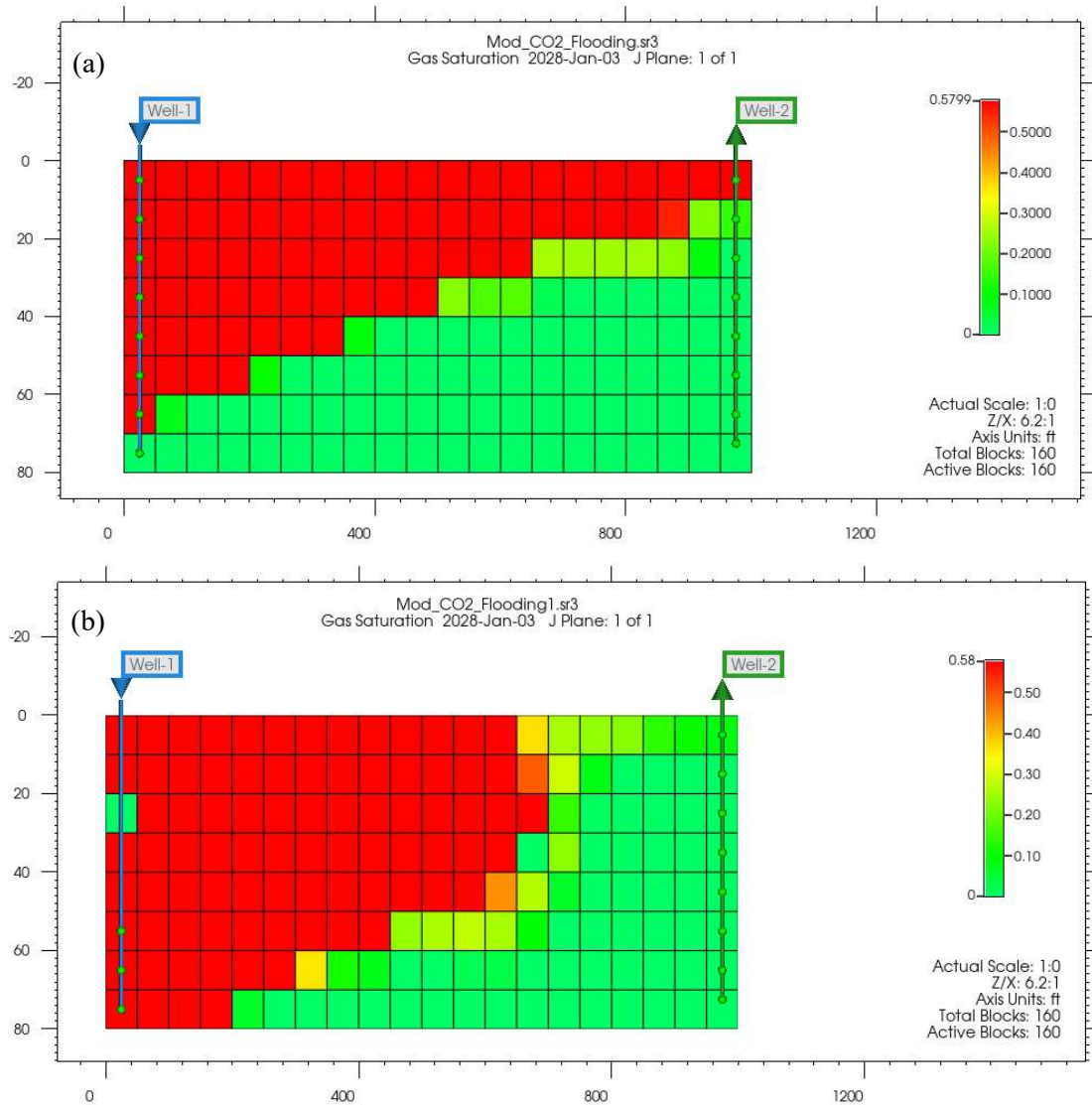
Figure 10. Gas saturation profile during gas injection from (a) all zones, (b) lower zones

5.4. Effect of Vertical to Horizontal Permeability Ratio

Vertical permeability controls vertical flow of reservoir fluids as well as the injected fluid. The effect of the ratio of vertical to horizontal permeability was therefore evaluated through simulation results. The simulation results of waterflooding and CO_2 gas injection with constant horizontal permeability (50md) and different vertical permeability (50 md and 10 md) are reported through water and gas saturation profiles. From Figure 11, with low vertical permeability (10 md) there is an increase of volumetric sweep efficiency of water displacing oil during waterflooding. In fact, volumetric sweep efficiency is increased with low vertical to horizontal permeability ratio because water injected from the upper zones can relatively flow horizontally.
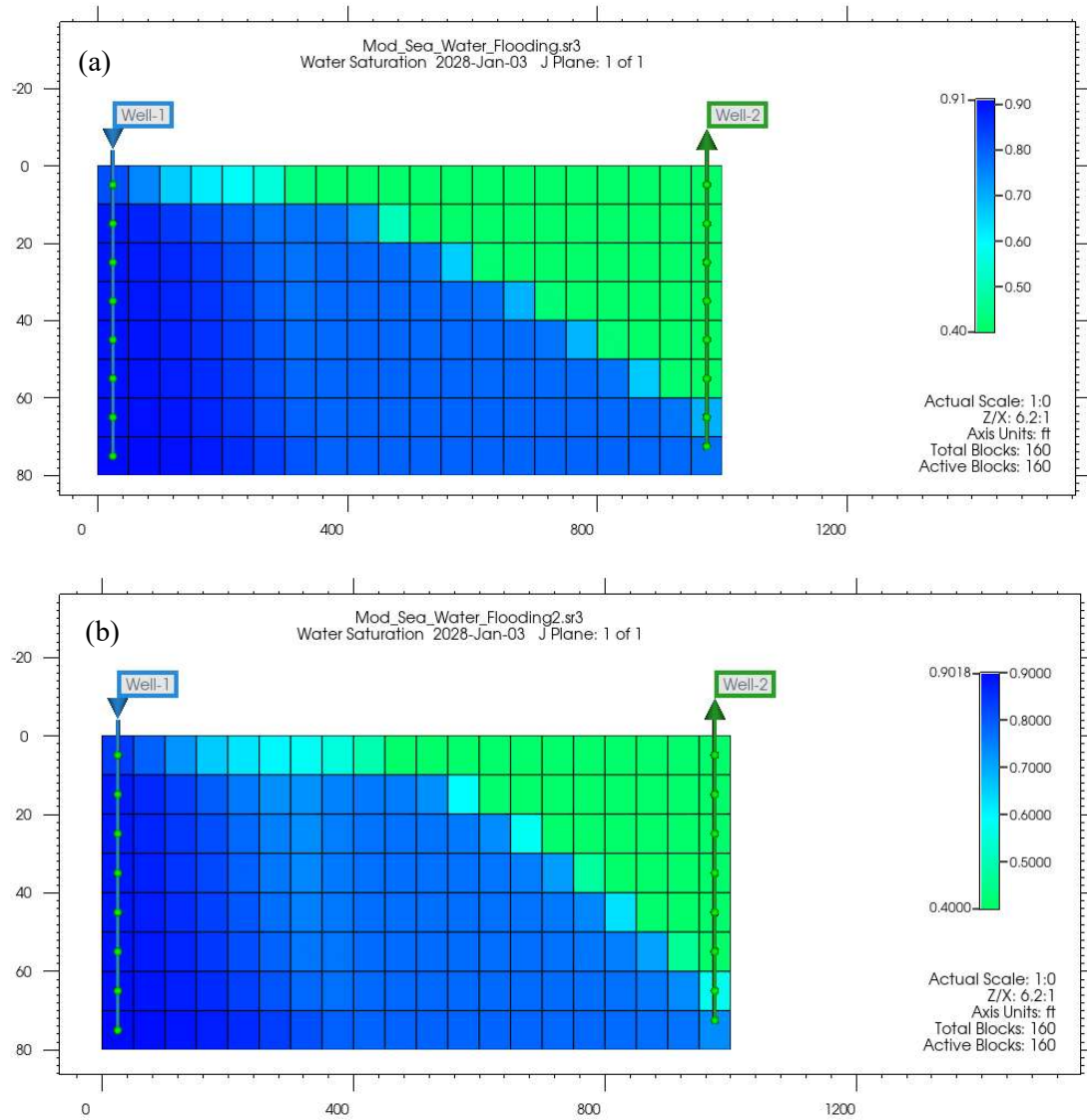
Figure 11: Water saturation during waterflooding with vertical permeability of (a) 50 md and (b) 10 md

In Figure 12, lowering the vertical permeability increases the frontal displacement of oil by gas injection in lower and middle zones of the reservoir while also controlling the early gas break through from the upper zones of the reservoir.
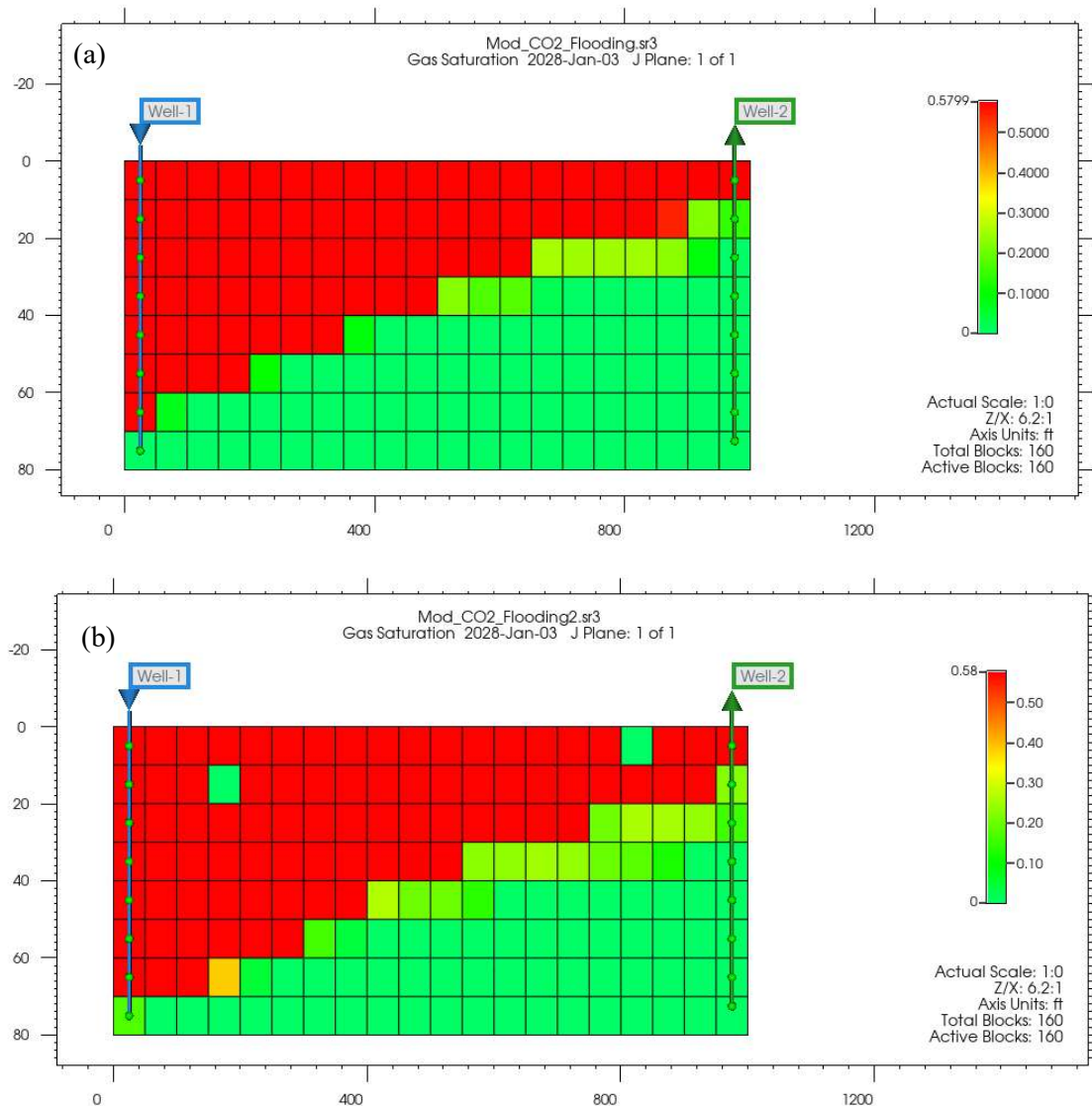
Figure 12. Gas saturation during CO_2 gas injection with vertical permeability of (a) 50 md and (b) 10 md

5.5. Conventional WAG injection

In both cases of separate waterflooding and CO_2 gas injection, there are eventually water and gas breakthrough from lower and upper zones of the reservoir respectively while there remains a sizable region un-swept. It is therefore for this reason that the combination of water and gas was proposed and applied to produce the attic oil that remains in the case of only waterflooding and oil in lower zones in the case of only gas injection. After analysis of effects of gravity, initial oil phase, injection depth, and vertical to horizontal permeability ratio on individual waterflooding and CO_2 gas injection; the favorable conditions were applied for WAG injection simulation.

The initial single phase of oil was considered as it produced higher oil recovery percentage. The gravity effect during WAG injection is the most obvious because of density differences between water, oil, and gas. The waterflooding from the upper zones and CO_2 gas injection from the lower zones of the reservoir was also applied. In addition, the vertical permeability of 10 md and horizontal permeability of 50 md were used for WAG injection. As results, it is

shown in Figure 13 that the combination of water and gas is more efficient for increasing the sweep area and consequently increases the oil recovery.
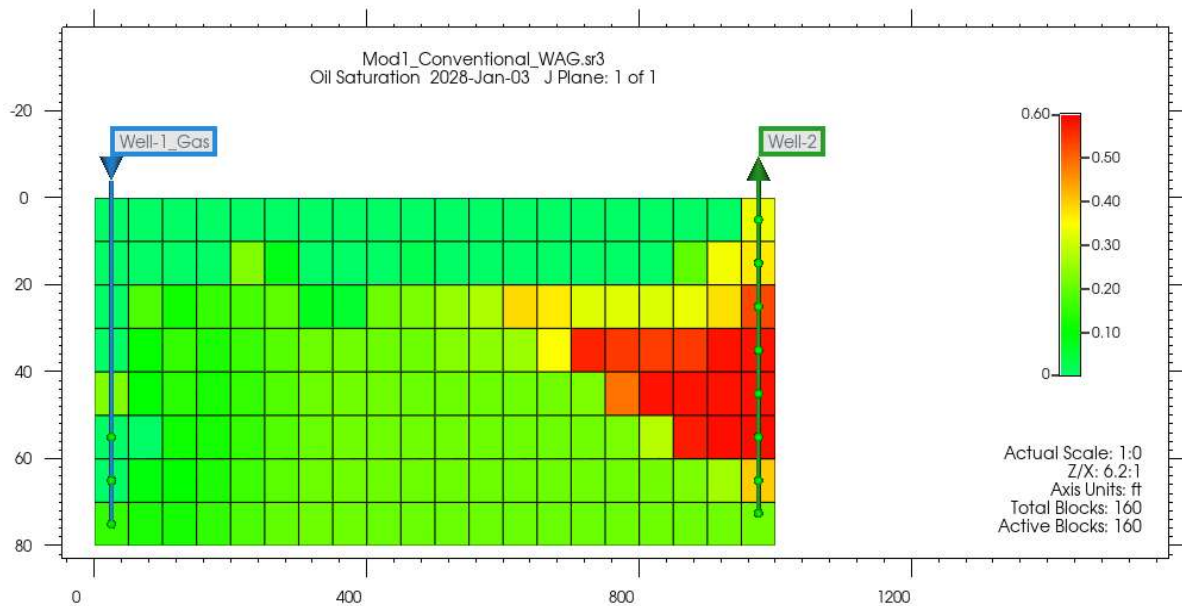
Figure 13. Frontal displacement of oil during WAG injection

Figure 14 shows the comparison of oil recovery factor for waterflooding, CO_2 gas injection and conventional WAG injection. The WAG injection increased oil recovery factor by about 10% from individual waterflooding and CO_2 gas injection. This result is explained by the fact that the combination of water and gas improves both macroscopic oil sweep and oil displacement efficiencies respectively. In fact, water displace oil from side-bottom and hence improve the macroscopic oil sweep efficiency. On the other hand, the CO_2 gas increases oil mobility by reducing its viscosity and hence it improves the oil displacement efficiency.
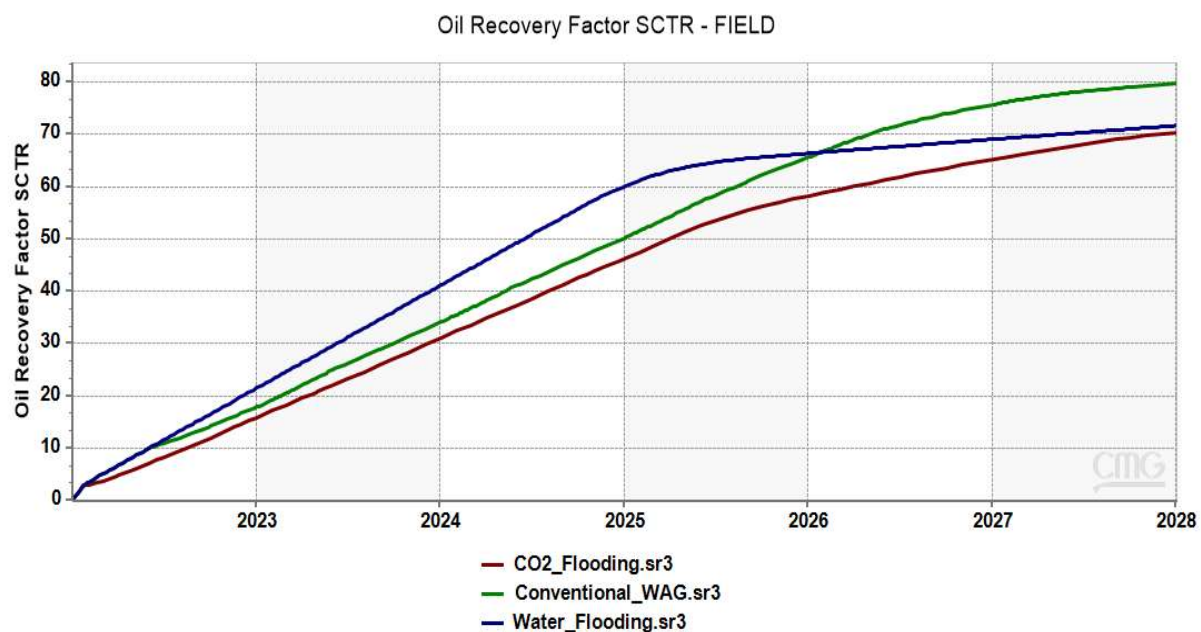

Figure 14. Advantage of WAG injection over continued waterflooding and CO_2 gas injection

5.6. Low Salinity Waterflooding (LSWF)

The effect of salinity of injected water was also evaluated through the results from a series of waterflooding by tunning its salinity. From the simulation results of different waterflooding scenarios as shown in Figure 15, there is an increase of about 8% of oil recovery factor from simulation with sea water of 51346ppm to simulation with low salinity of 1026.9ppm. In addition, the results show that low salinity and completely deionized waterflooding provide the same oil recovery factor. It means that the necessary dissolution of clay minerals for optimum oil recovery is achieved with low salinity of 1026.9ppm.
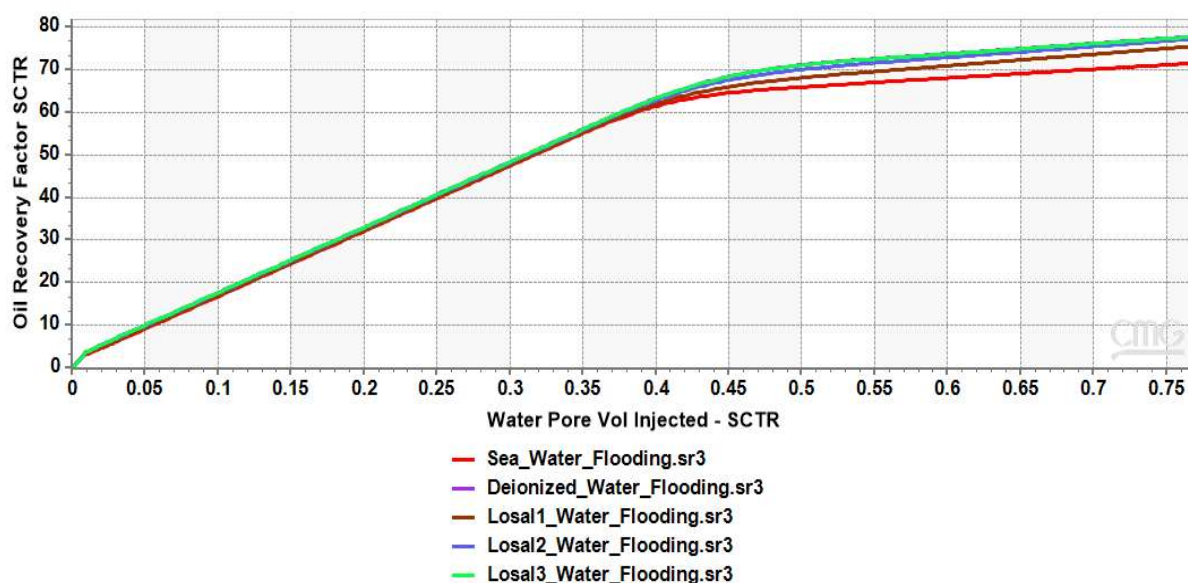
Figure 15. Oil recovery factor from different simulation scenarios of low salinity waterflooding

This increase of oil recovery factor by decreasing water salinity is attributed to the multi-ion exchange and mineral reactions that take place when low salinity water is injected into the rock containing clay minerals. There is wettability alteration from oil wet to preferred water wet when low salinity water is injected. In fact, the multi-ion exchange and wettability alteration are the two main mechanisms that oil is freed from pores and displaced by water in the case of LSWF. In addition, low salinity waterflooding increases oil recovery by breaking the rock-brine-oil interfacial tension. So, there is dissolution of rock minerals like calcite and dolomite which respectively release Ca^{2+} and Mg^{2+} with carboxyl complex in a multi-ion exchange during low salinity waterflooding.

On contrary, high salinity waterflooding results no wettability change instead there is more of ion adsorption. The adsorption of divalent ions like Ca^{2+} on clay surface creates a strong interfacial tension between oil and clay surface.

5.7. Conventional WAG vs LSWAG

The combination of waterflooding and gas injection while also focusing on the effect of salinity content in injected water was evaluated and the performances of conventional WAG and LSWAG injections were compared. The simulations results of conventional and LSWAG injections showed that the combination of waterflooding from upper zones and CO_2 gas injection from lower zones of the reservoir, and reducing vertical to horizontal permeability ratio improves significantly the total sweep efficiency. The contribution of CO_2 gas injection in

improving the oil displacement was observed for both conventional WAG and LSWAG injections. The waterflooding contributed on improving the volumetric sweep efficiency in both cases but low salinity content in LSWAG injection particularly increases microscopic sweep efficiency due to multi-ion exchange. In other words, the increase of oil recovery factor by LSWAG injection is mainly attributed to multi-ion exchange and wettability alteration processes that take place during low salinity waterflooding. From the graphs in Figure 16, LSWAG injection produced higher oil recovery factor up to 6% more than sea water or conventional WAG after 6 years.
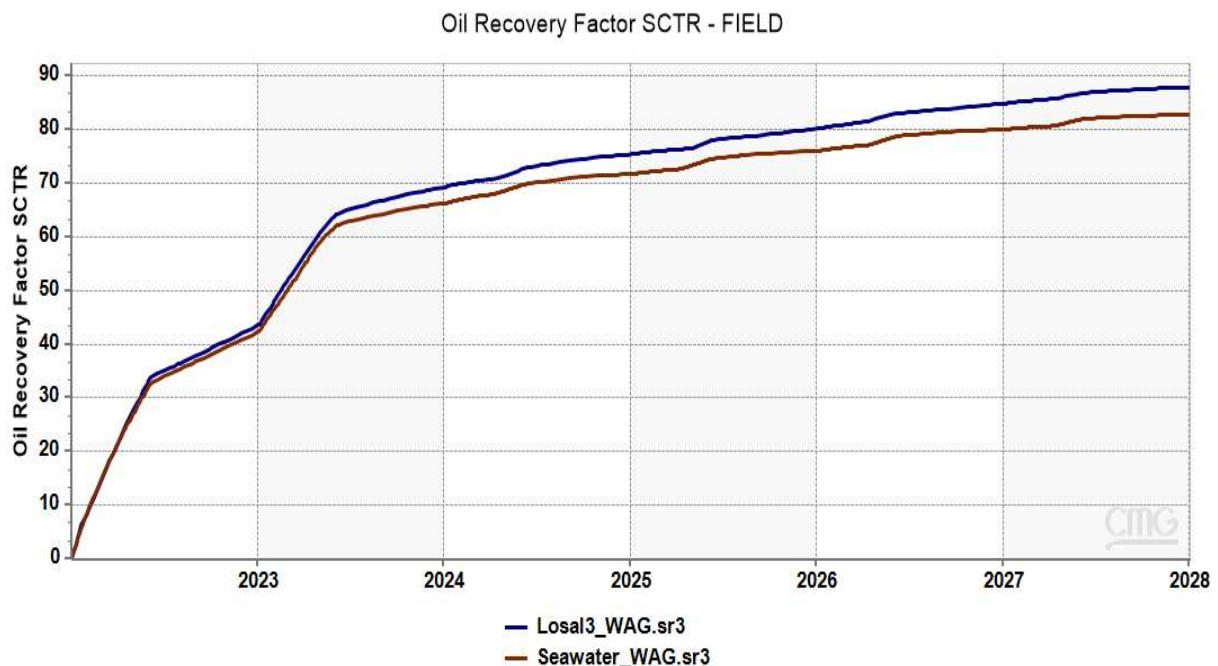
Figure 16. Comparisons of oil recovery factor from conventional WAG and LSWAG with maximum oil flow rate of 500bbl/day.

6. Conclusions

The effect of initial phase of crude oil, gravity, injection depth, and vertical permeability were considered and adjusted to minimize water and gas breakthrough while improving oil recovery factor during waterflooding, CO_2 gas flooding and WAG injection. The application of conventional WAG injection and LSWF individually was a success in improving oil recovery. However, this study showed that the combination or hybrid of the two methods improve further oil recovery for a typical sandstone reservoir. The effect of LSWF on releasing and displacing oil from pore surfaces is described through different mechanisms mainly wettability alteration and multi-ion exchange.

A series of simulation runs of different scenarios of waterflooding, CO_2 gas flooding, and WAG injection were performed by using CMG-GEM simulator. After the results were discussed and analyzed; the following conclusions were drawn:

1. The conventional WAG injection is the combination mechanism of waterflooding and gas injection that was invented to improve individual method of oil recovery. During WAG process, the oil sweep efficiency increases from individual waterflooding and gas injection, and as a result oil recovery factor increases. In this study, an increase of about 10% of oil recovery factor by conventional WAG injection to continued classical waterflooding and CO_2 gas injection was observed.

2. The oil recovery factor is higher with oil initially in single phase (liquid) than in two phases (liquid-gas) due to high gas to oil ratio for oil initially in two liquid-gas phases.
3. The waterflooding from upper zones and gas injection from lower zones of reservoir increase oil sweep efficiency and also prevent early breakthrough of injected fluids.
4. The low vertical to horizontal permeability ratio while injecting gas from lower zones and water from upper zones increases further the sweep efficiency as horizontal flow of water in upper layers and gas in lower layers respectively improve.
5. The water salinity effect was observed while comparing oil recovery factors from simulations of conventional WAG and LSWAG. There is up to about 6% increase of oil recovery factor from conventional WAG with sea water with salinity of 51,346 ppm to LSWAG with diluted sea water with salinity of 1027ppm.

Authors Statement

The authors confirm contribution to the paper as follows: study conception and design: Emmanuel Bucyanayandi, Muhammed Said Ergül, Ibrahim Kocabaş; data collection, analysis and interpretation of results: Emmanuel Bucyanayandi; draft manuscript preparation: Emmanuel Bucyanayandi, Ibrahim Kocabaş. All authors reviewed the results and approved the final version of the manuscript.

Conflict of Interest

The authors declare no conflict of interest.

References

Alpak, F. O., Lake, L. W., and Embid, S. M. (1999), "Validation of a Modified Carman-Kozeny Equation To Model Two-Phase Relative Permeabilities," *SPE Annual Technical Conference and Exhibition*, Houston, Texas.

Behrenbruch, P., & Goda, H. M. (2006), "Two-Phase Relative Permeability Prediction: A Comparison of the Modified Brooks-Corey Methodology with a New Carman-Kozeny Based Flow Formulation," *Proceedings - SPE Asia Pacific Oil and Gas Conference and Exhibition 2006: Thriving on Volatility*, 2, 810–827.

Bernard, G. G. (1967), "Effect of Floodwater Salinity on Recovery Of Oil from Cores Containing Clays," *38th Annual Calfornia Regional Meeting of the Society of Petroleum Engineeers*, California, USA.

Bonder P. (2010), "EOR-the time is now: Its contribution of world energy supply," *Society of Petroleum Engineers, Distinguished Lecturer Program*.

Brooks, R. H., & Corey, A. T. (1964), "Hydraulic properties of porous media," *Hydrology Papers*, 3, 1–37.

Buckley, J. S., Takamura, K., & Morrow, N. R. (1989), "Influence of Electrical Surface Charges on the Wetting Properties of Crude Oils," *SPE Reservoir Engineering*, 4(03), 332–340.

Dang, C. T. Q., Nghiem, L. X., Chen, Z., & Nguyen, Q. P. (2013), "Modeling Low Salinity Waterflooding: Ion Exchange, Geochemistry and Wettability Alteration," *Proceedings - SPE Annual Technical Conference and Exhibition*, 6, 4302–4323.

Dang, C., Nghiem, L. X, Nguyen, N., Chen, Z., & Nguyen, Q. P. (2015), "Modeling and Optimization of Low Salinity Waterflood," *Society of Petroleum Engineers - SPE Reservoir Simulation Symposium 2015*, 1, 55–73.

Dang, C., Nghiem, L. X, Nguyen, N., Chen, Z., & Nguyen, Q. P. (2016), "Mechanistic Modeling of Low Salinity Water Flooding," *Journal of Petroleum Science and Engineering*, 146, 191–209.

Delshad, M., Kong, X., Tavakoli, R., Hosseini, S. A., & Wheeler, M. F. (2013), "Modeling and Simulation of Carbon Sequestration at Cranfield Incorporating New Physical Models," *International Journal of Greenhouse Gas Control*, 18, 463–473.

Egbe, D. I. O., Jahanbani Ghahfarokhi, A., Nait Amar, M., & Torsæter, O. (2021), "Application of Low-Salinity Waterflooding in Carbonate Cores: A Geochemical Modeling Study," *Natural Resources Research*, 30(1), 519–542.

Gaines, G. L., & Thomas, H. C. (1953), "Adsorption Studies on Clay Minerals. II. A Formulation of The Thermodynamics of Exchange Adsorption," *The Journal of Chemical Physics*, 21(4), 714–718.

Hamouda, A. A., & Valderhaug, O. M. (2014), "Investigating Enhanced Oil Recovery from Sandstone by Low-Salinity Water and Fluid/Rock Interaction," *Energy and Fuels*, 28(2), 898–908.

Hosseini, S. A., Lashgari, H., Choi, J. W., Nicot, J. P., Lu, J., & Hovorka, S. D. (2013), "Static and Dynamic Reservoir Modeling for Geological CO2 Sequestration at Cranfield, Mississippi, U.S.A.," *International Journal of Greenhouse Gas Control*, 18, 449–462.

Hovorka, S. D., Choi, J. W., Meckel, T. A., Trevino, R. H., Zeng, H., Kordi, M., and Nicot, J. P. (2008), "Comparing Carbon Sequestration in an Oil Reservoir to Sequestration in a Brine Formation—Field Study," *9th International Conference on Greenhouse Gas Control Technologies (GHGT-9)*, 1(1). Washington, D.C.

Hustad, O. S., & Holt, T. (1992), "Gravity Stable Displacement of Oil by Hydrocarbon Gas After Waterflooding," *Eighth Symposium on Enhanced Oil Recovery, Tulsa: Society of Petroleum Engineers (SPE)*.

Jerauld, G. R., Lin, C. Y., Webb, K. J., & Seccombe, J. C. (2008), "Modeling Low-Salinity Waterflooding," *SPE Reservoir Evaluation & Engineering*, 11(06), 1000–1012.

Knappskog, O. A. (2012), "Evaluation of WAG injection at Ekofisk," M.Sc. Thesis, *University of Stavanger*, Norway.

Lu, J., Kharaka, Y. K., Thordsen, J. J., Horita, J., Karamalidis, A., Griffith, C., and Hovorka, S. D. (2012), "CO2–Rock–Brine Interactions in Lower Tuscaloosa Formation at Cranfield CO2 Sequestration Site, Mississippi, U.S.A.," *Chemical Geology*, 291, 269–277.

McGuire, P. L., Chatham, J. R., Paskvan, F. K., Sommer, D. M., & Carini, F. H. (2005), "Low Salinity Oil Recovery: An Exciting New EOR Opportunity for Alaska's North Slope," *SPE Western Regional Meeting, Proceedings*, 439–453.

Mississippi Oil and Gas Board (1966), Cranfield Field, Cranfield Unit, basal Tuscaloosa Reservoir, Adams and Franklin Counties. Jackson Mississippi.

Modelling of Low Salinity Water Flooding using STARS and GEM | Computer Modelling Group Ltd. (n.d.). Retrieved June 24, 2022, from https://www.cmgl.ca/training/modelling-low-salinity-water-flood.

Muggeridge, A., Cockin, A., Webb, K., Frampton, H., Collins, I., Moulds, T., & Salino, P. (2014), "Recovery Rates, Enhanced Oil Recovery and Technological Limits," *Philosophical Transactions of the Royal Society A: Mathematical, Physical and Engineering Sciences*, 372.

Qiao, C., Li, L., Johns, R. T., & Xu, J. (2015), "A Mechanistic Model for Wettability Alteration by Chemically Tuned Waterflooding in Carbonate Reservoirs," *SPE Journal*, 20(4), 767–783.

Soong, Y., Howard, B. H., Dilmore, R. M., Haljasmaa, I., Crandall, D. M., Zhang, L., and Mclendon, T. R. (2016), "CO2/Brine/Rock Interactions in Lower Tuscaloosa Formation," *Greenhouse Gases: Science and Technology*, 6(6), 824–837.

Srisuriyachai, F., & Muchalintamolee, N. (2014), "Cation Interference in Low Salinity Water Injection in Sandstone Formation," *76th European Association of Geoscientists and Engineers Conference and Exhibition 2014: Experience the Energy - Incorporating SPE EUROPEC 2014*, 2014(1), 3565–3569.

Stancliffe, J. R., & Adams, R. E. (1986), "Lower Tuscaloosa Fluvial Channel Styles at Liberty Field, Amite County, Mississippi," *Gulf Coast Association of Geological Societies Transactions*, 36, 305–313.

Tang, G. Q., & Morrow, N. R. (1999), "Influence of Brine Composition and Fines Migration on Crude Oil/Brine/Rock Interactions and Oil Recovery," *Journal of Petroleum Science and Engineering*, 24(2–4), 99–111.

Teklu, T. W., Alameri, W., Kazemi, H., Graves, R. M., and AlSumaiti, A. M. (2017), "Low Salinity Water–Surfactant–CO2 EOR," *Petroleum*, 3(3), 309–320.

Touray, S. T. (2013), "Effect of Water Alternating Gas Injection on Ultimate Oil Recovery," M.Sc. Thesis, *Dalhousie University*, Halifax, Nova Scotia, Canada.

Zitha, P., Felder, R., Zornes, D., Brown, K., and Mohanty, K. (2011), "Increasing Hydrocarbon Recovery Factors," *Society of Petroleum Engineers*.